Relative Tensile Strengths of Chainmail Weaves

By

Antonia J.N. Warner

Submitted to the
Department of Mechanical Engineering
in Partial Fulfillment of the Requirements for the Degree of

Bachelor of Science in Mechanical Engineering

at the

Massachusetts Institute of Technology

June 2015

© 2015 Antonia J.N. Warner. All rights reserved.

Signature of Author: __ **Signature redacted**

Department of Mechanical Engineering
May 19, 2015

Certified by: **Signature redacted**

Dr. Susan Brenda Swithenbank
Lecturer in Mechanical Engineering
Thesis Supervisor

Signature redacted

Accepted by: _____

Anette Hosoi
Professor of Mechanical Engineering
Undergraduate Officer

Relative Tensile Strengths of Chainmail Weaves

By

Antonia J.N. Warner

Submitted to the Department of Mechanical Engineering
on May 19th in partial fulfillment of the requirements for the degree of
Bachelor of Science in Mechanical Engineering

Abstract

Chainmail is a type of body armor that has been used throughout ancient and modern times by a variety of people, including medieval fighters and ocean divers. Articles of chainmail are made out of interconnected metal rings – usually steel rings – that are either butted, welded, or riveted together. The primary failure mechanism of a piece is usually the rings being pried apart by a wedge-shaped object, such as the tip of a sword or a shark tooth. The ability of an article of chainmail to resist such failures depends on a variety of variables including the method of closure of the rings, the diameter and gauge of the rings used, and the weave type.

The relative strengths of different types of chainmail were investigated by conducting tensile tests on both physical and simulated samples. Eight different ring diameters, four different ring gauges, four different weaves, and three methods of closure of the rings (butting, riveting, and welding) were tested. For both methods of analysis, force-displacement curves were generated for each sample, and the yield forces, maximum forces, and effective elastic moduli extracted from the graphs.

Proportional relationships between the physical characteristics of the chainmail and the forces and moduli were obtained graphically through analysis of the experimental data. The yield and maximum forces were determined to vary directly with the number of rings linked to a given ring, with an average error of 10.66 ± 5.67 %. These parameters were also found to vary inversely with the ring diameters, with an average percent error of 14.63 ± 5.61 %. The samples with welded rings were found to yield at a force at least 1.5 times higher than the yield force of the riveted samples and at a force at least 2 times higher than the yield force of the butted samples. The effective elastic moduli decreased with increasing diameter and held relatively constant across the different methods of ring closure. The attempt to scale the forces and moduli with the cross-sectional area of the rings proved inconclusive due to large percent differences between the scaled values.

The experimental results were compared to those generated by nonlinear, dynamic SolidWorks simulations. The verification of the simulated results with the experimental results allowed investigation into possible sources of error in the experimentation via simulation. Variations in the orientation of the rings resulted in variations in the yield force up to 33.31%. The yield force was also found to decline as a rate of 100 N for each millimeter of width of the split in the butted rings. Thus, the simulations provided possible explanations for some of the larger percent differences found during the creation of the proportional relationships – including the inconclusive results for scaling with cross-sectional area. Despite the possibilities for error, there exists strong support for the scaling relationships established for weave type and ring diameter due to the low percent errors calculated, as well as the low percent errors between the simulated and experimental values.

Thesis Supervisor: Susan B. Swithenbank
Title: Lecturer in Mechanical Engineering

Acknowledgements

I would like to thank my thesis supervisor Dr. Susan Swithenbank for her continued support and mentorship throughout this project. Additionally, I would like to thank Pierce Hayward for providing the tensile testing set-up and James Hunter for making the forge-welded samples. I would also like to thank Dr. Barbara Hughey and Jared Berezin for their help in editing and creating graphics. Finally, I would like to thank Ashin Modak for his help in trouble-shooting problems with the SolidWorks simulations, as well as Pavlina Karafillis for accompanying me to lab at late hours to ensure my continued survival.

Table of Contents

List of Figures

List of Tables

1. Introduction

Chainmail is a type of body armor that has been used across the centuries by a variety of people, including medieval fighters on the field of battle and modern divers in shark-infested waters. Although a chainmail suit cannot protect effectively against impact, it prevents the wearer from sustaining open wounds and allows for more fluid movements, unlike other types of protection like medieval plate armor [1]. The flexible and yet slash-resistant properties of chain mail arise from the fact the suits are made out of interconnected iron, steel, or bronze rings. Due to the fact that objects such as swords are made out of similar or weaker alloys, chainmail is rarely damaged through cutting. Instead, the primary form of failure of chainmail suits is usually the rings being wrenched open [1]. Such failures can be caused by a variety of factors, including sustained or high impulse loading from the weight of the suit or being pried apart by the wedge-shaped tip of a sword or a shark tooth.

The relative strengths of different types of chainmail were investigated by inducing failure of a sample via both an experimental tensile test and simulated tensile test. Tensile tests are analogous to the failure mechanism of the rings in which wedge-shaped objects force the rings open as they penetrate the open center of the rings. The method of construction used to create an article of chainmail determines both its ability to withstand failure and the rate at which it fails. The primary variables in the construction of chainmail are the ring material, the diameter of the rings, the cross-sectional area of the wire used to make the rings, the method of closure of the rings, and the weave pattern. To discover the impact that each of these variables have on the strength of chainmail, the effective elastic moduli, yield forces, and maximum forces were found for each of the samples tested by creating force-displacement curves from tension test data.

The raw data collected from the experimental tension tests was analyzed to make qualitative statements about the impact of the physical parameters of the chainmail on its strength. Following this, an attempt was made to correlate the trends in the values of the Young's moduli, yield forces, and maximum forces of the samples to the ring and weave parameters. The accuracy of these correlations can be visualized via the percent differences between appropriately scaled force and elastic modulus values. These values and percentages can be used to comment on the relative strengths of different weave types and rings, and predict the behavior of other samples.

A series of SolidWorks simulations was conducted to verify the results achieved through the experimental tension tests; the non-linear, dynamic simulations output yield force and effective elastic modulus values that were compared to those found experimentally. In addition to being used to verify the outputs of the experimental tension tests, the simulations were used to investigate several possible sources of error in

the experimentation that arose from the configuration and construction of the physical chainmail samples. Thus, the simulations served to both provide further support to the data collected experimentally in tension tests and investigate the validity of the posited sources of error in the experiment.

2. Background

Methods of construction influencing the strength of a sample of chainmail include the type of metal used, the weave-type, and the method of closure of the rings. Values characterizing the strength of a sample are extracted from force-displacement graphs.

2.1 Chainmail Construction
2.1.1 Metals

The test samples are made out of two different types of metal: 1018 mild steel and galvanized 1018 mild steel. Mild steel contains 0.05% to 0.3% carbon by weight; the higher the carbon-content of the steel, the more resistant the steel is to bending and cutting [2]. Mild steel is low-carbon compared to many other forms of steel, and so is relatively low-strength steel. Some of the material properties of mild steel are contained in Table 2.1. Due to the less sophisticated metal-working capabilities of armorers in medieval times, mild steel rings were assumed to be the most accurate representation of the rings used in medieval chainmail. Galvanizing steel is a common practice in modern times for improving the anti-rusting properties of a piece of steel by coating it in zinc [3]. Galvanized mild steel is commonly used in modern forms of chainmail due to the added benefits of the galvanic coating, as well as the increase in the price of metal with increasing carbon content [1]. Studies conducted into the strength of steel have found that there is no significant difference between the strength properties of mild steel and galvanized mild steel [3]. Consequently, tests conducted using mild steel rings are directly comparable to tests conducted using galvanized mild steel rings.

Table 2.1: Material properties of mild steel [2].

	Young's Modulus [GPa]	Yield Strength [MPa]	Ultimate Strength [MPa]
1018 Mild Steel	205	283	365

2.1.2 Weaves

Mild steel and galvanized mild steel rings can be used to create chainmail samples with a variety of different weaves. Rings are made by winding wire around a rod with a specified outer diameter and cutting along the central axis of the rod to form split rings. Each of the rings is opened and closed and linked to other rings in a set of specified patterns to form a weave. The simplest weave is the chain, which has two rings inserted in each other ring, as shown in Figure 2.1. A slightly more complex version of

10

this weave is the spiral weave (Figure 2.2) which has four rings inserted in every other ring. Theoretically, the spiral weave should be twice as strong as the chain weave, due to the fact that the number of rings passing through each other ring is doubled.

Figure 2.1: A chain weave is characterized by each ring passing through two other rings. [5]

Figure 2.2: A spiral weave is characterized by each ring passing through four other rings. [6]

More complex types of weaves are used to create sheets of chainmail. The most commonly used type of sheet weave is the European four-in-one weave, the sub-unit of which is shown in Figure 2.3.1. The middle row in the sub-unit contains rings with four rings passing through each ring and the rows on the outside have only two rings passing through each ring. When sub-units are connected into a sheet, this weaker edge remains and will propagate as the piece tears. As a result, a sample of the European weave should theoretically only be as strong as the chain weave. Connecting the edges of the weave to form a cylinder will remove the existence of the weaker edge, such that each ring in the piece has four rings linked to it. When the European weave is folded and its two sides connected, as in Figures 2.3.2 and 2.3.3, the simplest form of such a cylinder is created (shown in 2.3.4). This weave, called the box weave, should be twice as strong as both its sub-unit (the European weave) and the chain weave, and of comparable strength to the spiral.

Figure 2.3: 2.3.1 shows the European four-in-one weave, which, when manipulated as shown in 2.3.2 and 2.3.3, will create the box weave shown in 2.3.4. The box weave will behave like a cylindrical sample of the European four-in-one weave. [7]

11

2.1.3 Methods of Closure

Once the rings are connected into the desired pattern, the method of closure is chosen. The simplest method of closure is to leave the samples as they are – with the ends of the rings butted up against one another as in Figure 2.4a. However, ancient and modern chainmail is commonly strengthened in one of two ways: welding or riveting. In the case of welded rings, the rings are welded closed once they have been connected into a piece of chainmail, as in Figure 2.4b. In the case of riveted rings, as shown in Figure 2.4c, the ends of the rings are flattened, have a hole punched through them, and a rivet secured through that hole after the rings have been connected into a weave.

a.   b.   c.
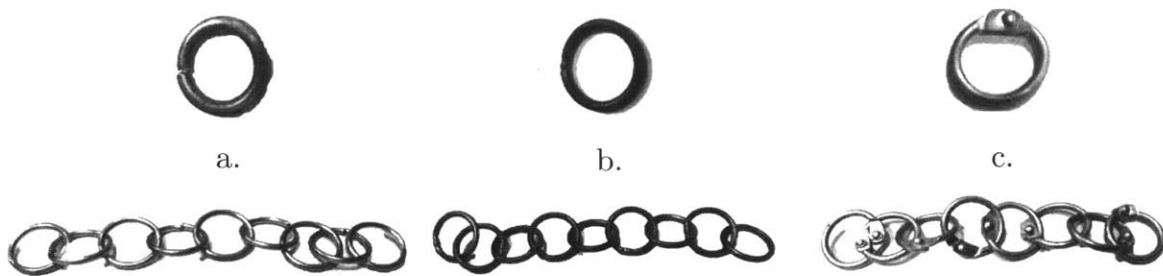
Figure 2.4: Images of ring and chain samples with different methods of closure of the rings. From left to right: butted (a), riveted (b), welded (c).

2.2 Force-Displacement Curves

Data collected from a tension test of a sample yields a force versus displacement graph, such as the one shown in Figure 2.5. A tensile test curve has several distinctive features revealing information about the strength of the sample, including its effective elastic modulus, the yield force, and the maximum force it can experience before failure.
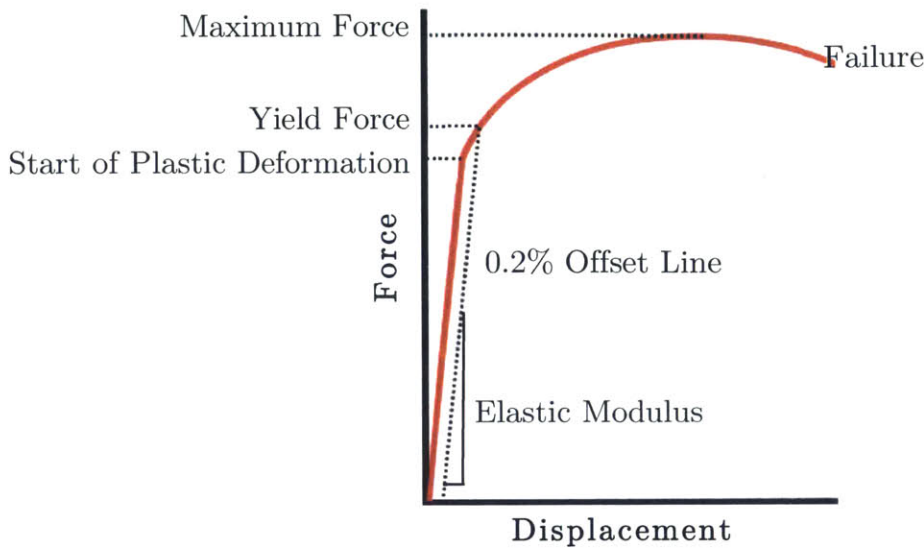
Figure 2.5: An example tensile testing curve for a relatively non-ductile material, showing features of interest including the transition from elastic to plastic deformation, the 0.2% Offset Yield Force, the Maximum Force, and the Failure Point.

The initial linear portion of the curve in Figure 2.5 represents the elastic regime of a sample under tension. The modulus of elasticity is an inherent material property that characterizes the stiffness of a sample, and is found from the slope of the elastic regime in a stress-strain curve [4]. An analog to this elastic modulus (henceforth referred to as the effective elastic modulus), with units of [N/mm] rather than [N/mm^2], is found from the slope of the linear portion of the force-displacement curve. For chainmail, the value of the effective elastic modulus varies based upon the ring diameter and gauge, as well as the length of the chain. The effect of the length of the chain on the relative size of the deformation of each of the samples can be minimized by choosing a set length in terms of the number of rings in the sample.

When the graph transitions from linear to non-linear, the sample enters the plastic regime, in which any imposed deformations are permanent [4]. The yield point of the material is commonly defined to be the point where the curved portion of the graph is intersected by a line with the same slope as the elastic regime, but with an x-intercept of 0.2% of the final deformation (instead of zero). The peak of the curved region is the maximum force that the material is able to undergo. After the maximum force is reached, the sample undergoes necking - a significant decrease in the cross-sectional area of the rings that results in a decrease in the force required for further plastic deformation to occur [4]. This period of necking is eventually followed by the failure of the sample.

The curve shown in Figure 2.5 is applicable for materials that undergo relatively little plastic deformation before failure. More ductile samples undergo not only significant necking but also significant strain hardening. Strain hardening is the process in which a material becomes more resistant to deformation as plastic deformation continues [4]. This increased strength is due to the fact that the material eventually becomes saturated with atoms dislocated by the deformation that impede both the creation of further dislocations and further lengthening of the sample [4]. An example of a force-displacement curve for a ductile sample is shown in Figure 2.6.
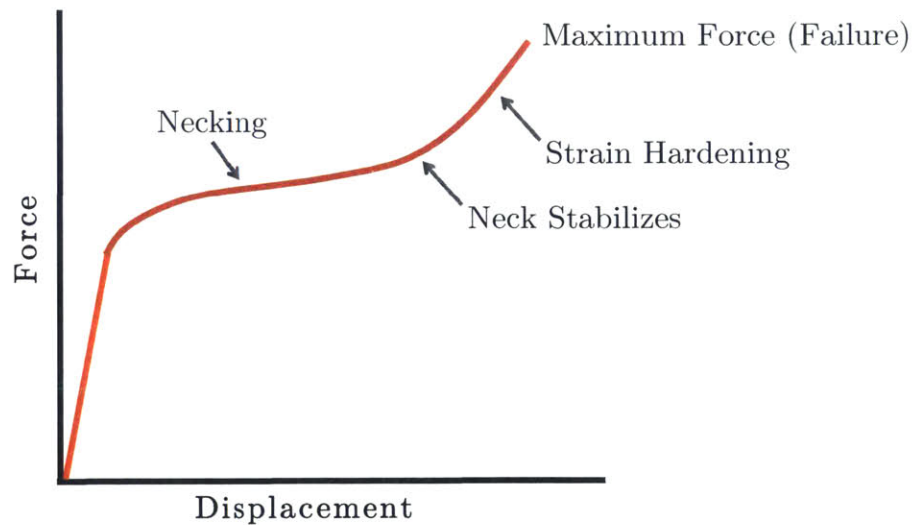
Figure 2.6: An example force-displacement graph for a relatively ductile material. The curve exhibits strain hardening in addition to an initial elastic regime, necking, and sample failure.

3. Methods and Experimental Set-Up

A variety of chainmail samples were created and placed in an INSTRON tensile testing machine, which induced a displacement until the sample broke into two pieces. SolidWorks simulations of chains with the same parameters as the physical samples were created to compare the experimental results with theoretical ones and investigate possible sources of error.

3.1 Sample Parameters

Galvanized, butted rings were used to investigate the relationship between the weave type and the yield and maximum forces. Samples of chain, spiral, European four-in-one, and box weaves made from 16-gauge wire rings with an inner diameter that was nominally ¼ inch were tested. The dimensional parameters of the 16-gauge wire rings were measured using calipers, and are shown in Table 3.1. Figure 3.1 illustrates the locations of the dimensions taken. Some variation in length occurred for the samples

14

being tested were connected to the top and bottom of each sample; this addition was made to ensure that the sample would not fail at the ring connected to the mount. A bolt was threaded through these rings on both ends of the sample and passed through a u-shaped mount on the INSTRON machine, as shown in Figure 8. A displacement of 0.05 mm/s was applied to the top fixture by the machine until the sample failed.
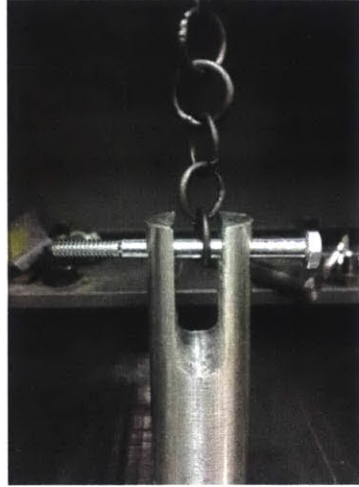
Figure 3.2: A sample chain held taught in the INSTRON machine by the mounting hardware used for the tensile tests.

3.3 Proportionality Relationships

The effective elastic modulus, yield force, and maximum force were found graphically for each of the samples from the force-displacement curves generated by the INSTRON machine. Conducting a set of three trials for each sample type yielded an average value for each of the force or effective elastic modulus values. To investigate how these average values varied with the parameters of the chainmail, each of the values was assumed to be proportional to some function of the physical characteristics of the weave or ring; the strength of the samples was hypothesized to vary with the number of rings connected to each other ring, the diameter of the rings, and the cross-sectional area of the wire. These relationships were investigated by creating a ratio between a measured value and one of the parameters for one sample type and comparing this ratio to that for another sample type. For example, in order to investigate how the yield force varied with diameter, the yield force found for a chain with one diameter of rings was divided by the ring diameter, and set equal to the ratio of a yield force and diameter found for another chain. The percent difference between the two ratios reflects the accuracy of the proportionality relationship created between the yield force value and diameter of the rings. Similar calculations were conducted that

17

compared the full set of yield forces, maximum forces, and effective elastic moduli with the physical parameters of the rings and weaves.

Slight differences between the diameters for different gauges that were nominally the same (ie. D1 for 12 gauge rings was slightly different from D1 for 14 gauge rings) added an additional level of complexity to the analysis of the impact of the ring gauge on sample strength. In order to correct for the impact that theses differences in diameter had on the strength of the rings, the proportional relationship found for ring diameter was used to appropriately scale the forces before using the force values to investigate variations with gauge. This scaling was implemented in order to improve the accuracy of the proportional relationship developed for ring gauge, but had the downside of introducing an additional source of error in these scalings.

3.4 SolidWorks Simulations

The SolidWorks simulations created for these experiments were made using the SolidWorks 2015 Simulation package. In order to account for the complex behavior of the samples, namely the ductility of the steel, the shape of the rings, and the high levels of plastic deformation, the chosen form of the simulations was non-linear and dynamic. Each of the tests was conducted for a set of two rings; the number of rings was limited due to the fact that the processing power of SolidWorks proved to not be capable of handling a system containing more rings without experiencing issues with the number of constraints that needed to be imposed on the system. Images of several solidworks models created, featuring different methods of ring closure, are shown in Figure 3.3.

Figure 3.3: SolidWorks models created for simulating butted, riveted, and welded rings. The splits, welds, and rivets were all oriented at 90° angles from the vertical, as this position is in the middle of the range of possible positions for these features. (a) Depicts a chain of 12-gauge, D2 rings with a gap size of 0.3 mm. (b) Depicts a set of welded 12-gauge, D2 rings with the weld 0.6 mm in width. (c) Depicts 14-gauge, D3 riveted rings with a rivet diameter of 0.7 mm.

A variety of constraints were placed upon the two-ring systems in the simulations. A feature with a flat face was added to the top of the higher ring and to the bottom of the lower ring. A close-up of this feature on the bottom ring is shown in Figure 3.4. Mates were added to fix Face 1 to to the top plane, Face 2 to the right plane, and Face 3 to the front plane. Additionally, in the simulation set-up, Face 1 was fixed and Faces 2 and 3 were constrained to only allow for vertical movements. The corresponding faces on the top ring were fixed to allow for only vertical, and not horizontal, movements. A linear mate was also created between the vertical diameter lines of the rings, along with a mate to keep the horizontal diameter lines perpendicular to one another. Finally, a non-penetration condition was estalished between the two rings in each of the simulations to prevent the rings from passing through one another as a force was applied to the top face of the flat feature on the top ring.
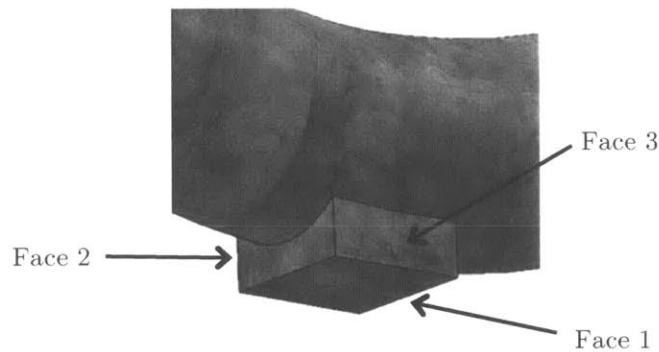
Figure 3.4: Close-up image of the feature added to each of the rings. The flat faces were used to apply fixtures to the rings in the simulations.

As with the physical samples, several dimensional parameters were varied between the simulations. For the butted-ring simulations, two diameters of a single gauge were tested and compared to results found experimentally. The experimental results for the riveted and welded samples were also verified using simulations of welded rings with three different diameters and of riveted rings with a single diameter (matching the dimensions of the physical samples). Simulations were also performed to investigate two potential sources of error in the butted ring experiments: the width of the gap in the rings and the orientation of the gap. Three different gap widths (0.001 mm, 0.3 mm, and 0.7 mm) and three ring orientations (shown in Figure 3.5) were tested.
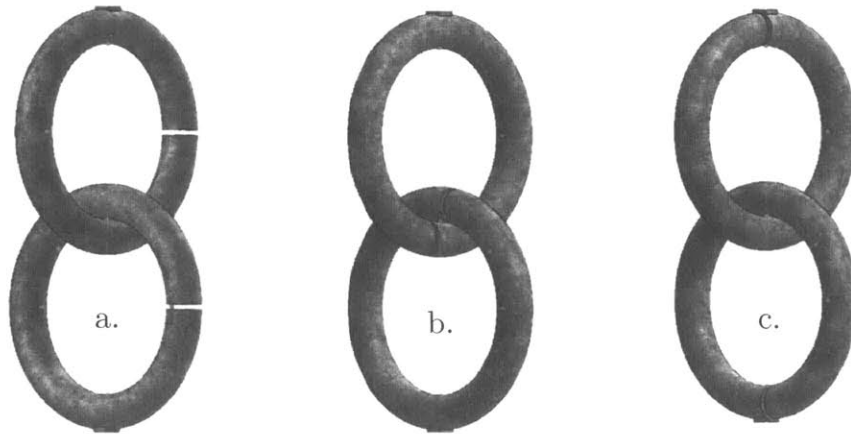
Figure 3.5: Images of the different split orientations tested for butted rings. (a) Split orientation used for all samples other than those in the investigation of the effect of split orientation on tension test results. Referred to as the 90° position. (b) Split orientation referred to as the 180° orientation. (c) Split orientation referred to as the 0° position. Degrees measurements were made relative to the flat features.

4. Force-Displacement Curve Examples

Force-displacement curves were created on the INSTRON machine for each of samples. Each of the curves generated followed the general shape of either of the expected curves shown in Figures 2.5 and 2.6. Variations in the shape of the curves from these expected curves occurred primarily in the case of variations in the weave type from the chain. The spiral, box, and occasionally European weaves exhibited multiple ring failures, the number of which depended on which of the rings failed. In the case of multiple failures, the curve leading up to the first failure was chosen for analysis, as the later failure points would not have exhibited the same elastic loading behavior due to the already deformed state of the sample. Examples of several of the force-displacement curves generated for different methods of ring closure are shown in Figures 4.1-4.3.
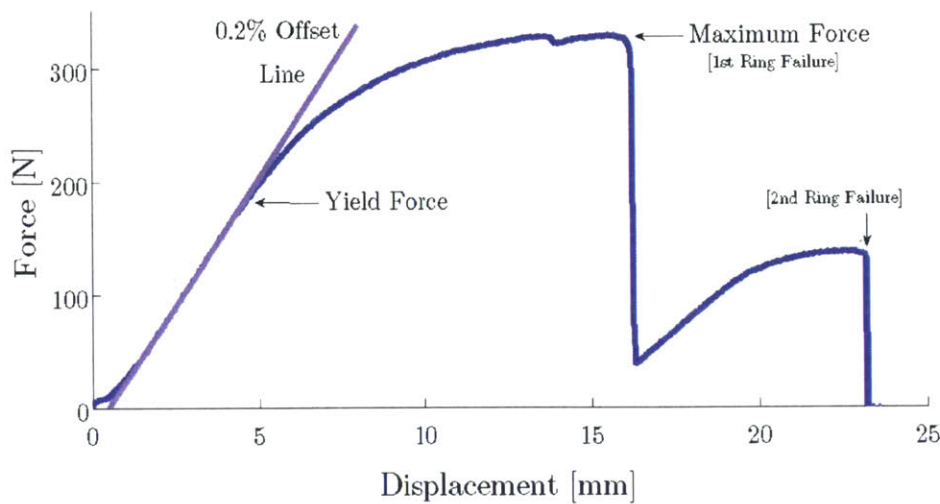
Figure 4.1: The blue curve is an example of a force-displacement curve generated for a box weave – in this case a box constructed from D3, 12 Gauge butted, galvanized rings. The linear fit created to find the elastic modulus and 0.2% Offset Yield is shown in purple. The multiple peaks evident in the blue line indicate that two rings failed before the whole sample broke. The second peak reaches a much lower maximum force, which is due to the fact that the ring that broke underwent both plastic and elastic deformation in the loading that resulted in the breakage of the first ring.
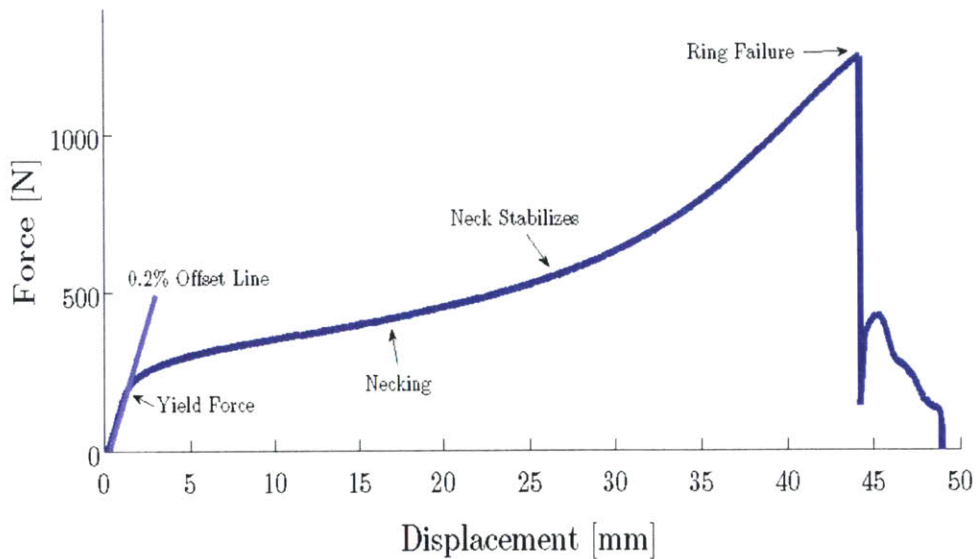
Figure 4.2: The blue curve is an example of a force-displacement curve generated for a welded chain constructed from D2, 16 Gauge mild steel rings. The linear fit created to find the effective elastic modulus and 0.2% Offset Yield is shown in purple. The weld strengthens the rings such that the neck is able to stabilize, leading the sample to experience more plastic deformation than that experienced by the butted rings. The rings failed at a variety of locations on the ring – not necessarily on the weld. Once failure had occurred, the then open rings continued to plastically deform and slip.
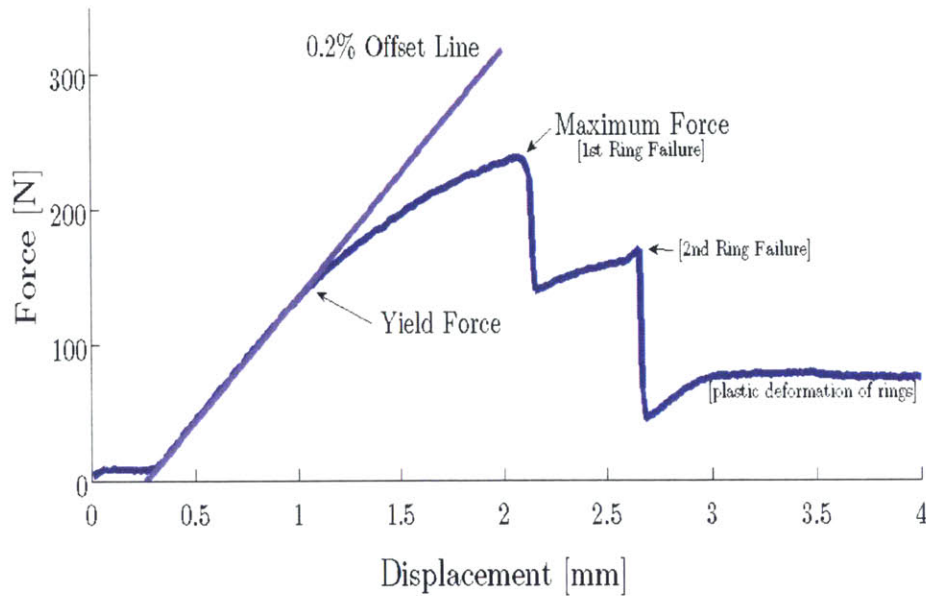
Figure 4.3: The blue curve is an example of a force-displacement curve generated for a riveted chain. The linear fit created to find the elastic modulus and 0.2% Offset Yield is shown in purple. The multiple peaks evident in the blue line indicate that two rivets failed before the rings underwent sustained plastic deformation.

5. Experimental Results and Discussion: Butted Rings

The INSTRON tensile testing machine generated force-displacement graphs that were analyzed for trends in the effective elastic moduli and maximum and yield forces. Proportional relationships were created between these values and various dimensional parameters of the rings, and percent differences calculated between the values attained in tests of different sample types.

5.1 Weave Type Results and Proportional Relationship

The yield and maximum force values were extracted from the force-displacement graphs for samples made from 16 gauge rings with four different weave types. The values shown in Figure 5.1 are the averages of the values found for the yield and maximum forces from three trials of each sample type. The difference in length between the samples of different weaves would not have impacted the yield and maximum forces, but would have impacted the effective Young's moduli. As a result, the differences between the effective Young's moduli for different weaves were not investigated. The force data appears to agree with the hypothesis that the yield and maximum forces increase as the number of rings passing through each other ring increases.
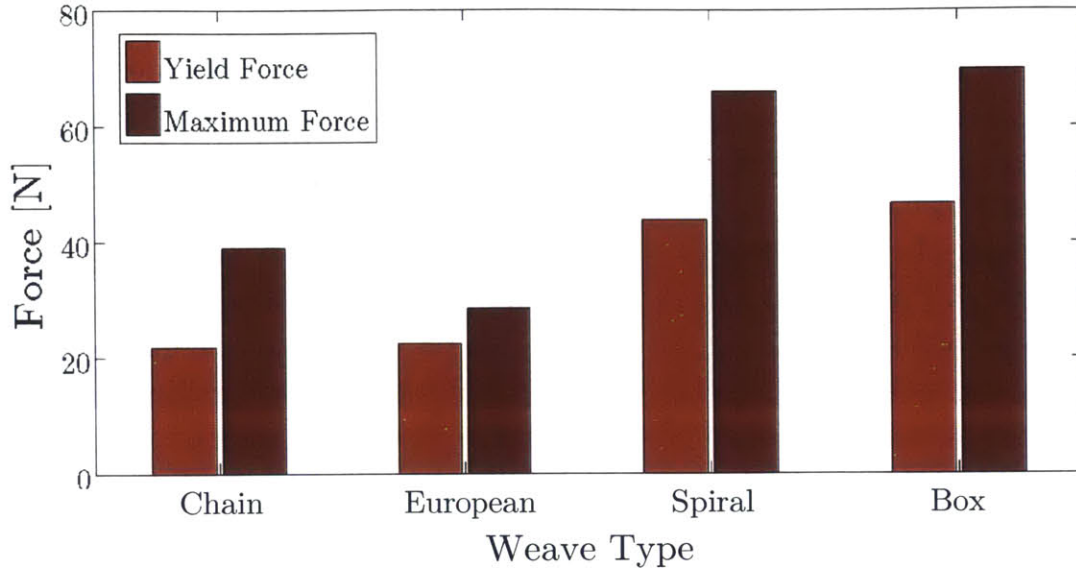
Figure 5.1: The yield force and maximum force values for chain, European, spiral, and box weaves. The hypothesis that weaves with two rings linked to each other ring (chain and European) will be half as strong as weaves with four rings linked to each other ring (spiral and box) appears to be supported.

The values of yield force and maximum force for different weaves were expected to scale with the number of rings passing through each ring in the weave. Therefore, it was hypothesized that the force values for the box and spiral weaves would be twice those for the chain and European four-in-one weaves. This expected scaling was investigated by dividing each of the force values by the number of rings linked to each ring, and finding the percent differences between the scaled maximum or yield force values for one weave and those for another weave. The percent differences generated are shown in Table 5.1.

Table 5.1: The percent differences between the scaled values of the yield or maximum forces for each of the weave types. Difference values below 10% (shown highlighted in green) are assumed to be accurate to within an acceptable margin of error. Difference values shown highlighted in red resulted from samples that failed more quickly than the other samples, and so the maximum force values tabulated are likely non-representative of the actual maximum values.

Weaves Compared	% Difference: Yield	% Difference: Maximum
Chain : European	2.90902	37.0760
Chain : Spiral	0.190476	18.473590
Chain : Box	6.03257	12.1316
Spiral : Box	5.85324	5.35304
Spiral : European	2.72374	15.7018
European : Box	3.21713	18.1975

The majority of the percent difference values comparing the scaled forces for the different weaves are below 10%. Additionally, the majority of the values not under 10% (shown in red) resulted from tests in which the rings underwent very little plastic deformation compared to the other samples tested. This lack of plastic deformation is likely due to the fact that if the splits in two of the butted rings happened to sit on top of one another, the breaks in the rings would have enabled the two rings to separate early on in the test. As a result, the maximum force values associated with these weaves are likely not indicative of the maximum forces that the samples are capable of withstanding before failure. Thus, Table 5.1 indicates with high probability that there is direct scaling in the yield and maximum force values with the number of rings passing through each other ring in the chainmail weave.

5.2 Diameter and Gauge Results
5.2.1 Yield Force Values

The yield forces extracted from the force-displacement graphs for each of the chains and boxes of 12, 14, and 16 gauge rings with different diameters are shown in Figure 5.2 and Figure 5.3 (respectively). Both chains and boxes were tested to verify that any relationships discovered for chains also held true for more complex weave types. Both of the yield force graphs for chain and box weaves support the hypothesis that as gauge or diameter increases (where increasing gauge means decreasing wire thickness) the yield force decreases.
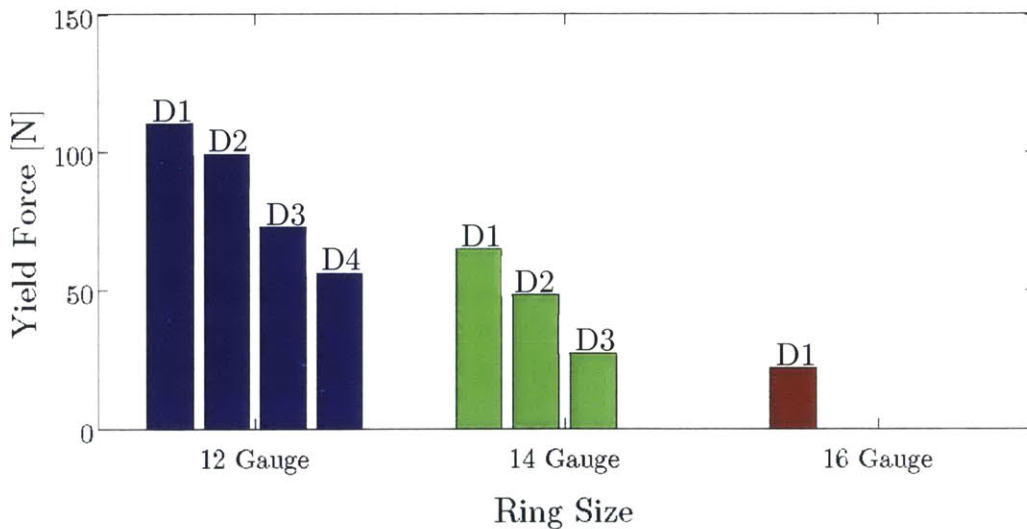
Figure 5.2: The relative yield forces for chains made from 12, 14, and 16 gauge rings at the four different diameters, with the diameters ranging from D1 to D4 from the left to right of each clustered group. There is a clear inverse relationship between increasing yield force and increasing diameter or gauge.
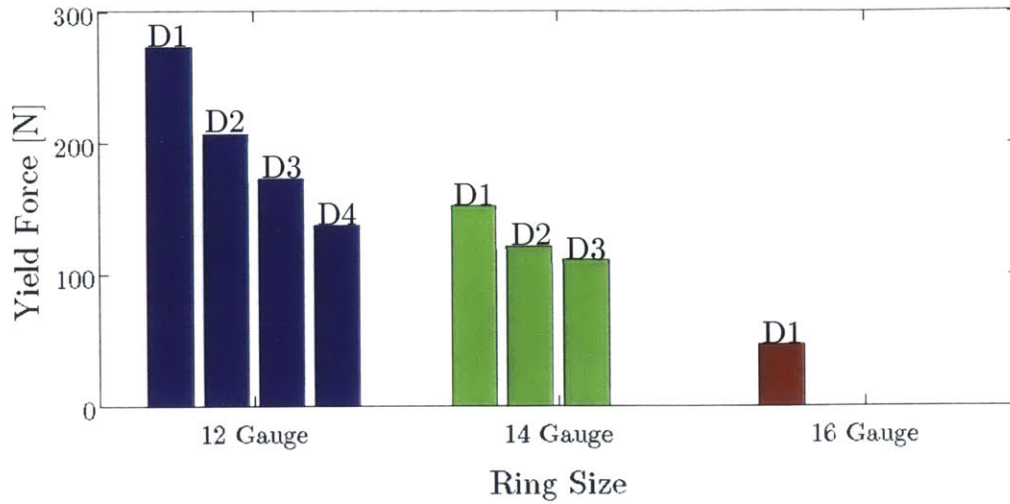
Figure 5.3: The yield forces for boxes made from 12, 14, and 18 Gauge rings at the four different diameters, with the diameters ranging from D1 to D4 from the left to right of each clustered group. This data for the box weaves provides support for an inverse relationship between increasing yield force and increasing diameter or gauge.

5.2.2 Maximum Force Values

The maximum forces extracted from the force-displacement graphs for each of the chains and boxes of 12, 14, and 16 gauge rings with different diameters are shown in Figure 5.4 and Figure 5.5 (respectively). The maximum force values exhibit the same trends as the yield force values, as an increase in gauge or diameter causes a decrease in maximum force.
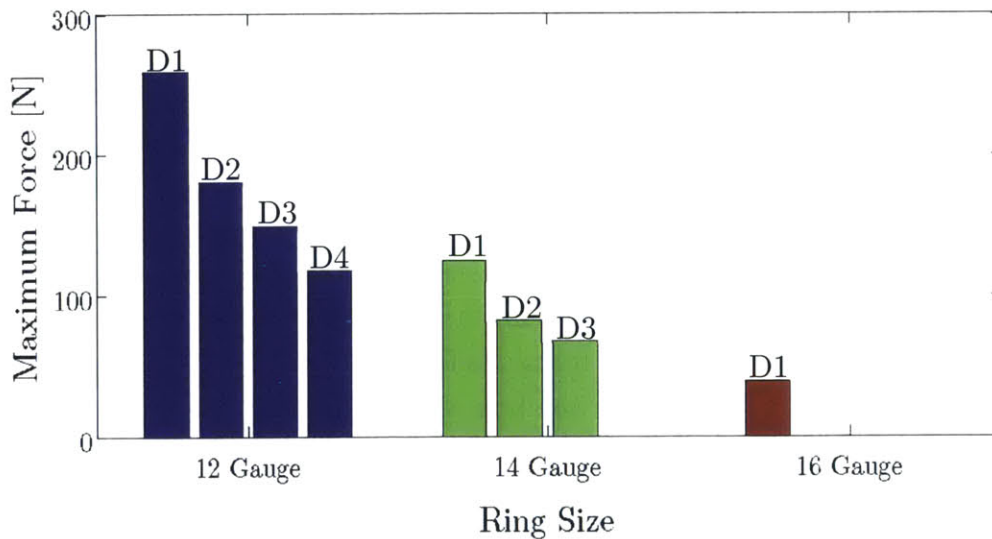
Figure 5.4: The relative maximum forces for chains made from 12, 14, and 16 Gauge rings at the four different diameters, with the diameters ranging from D1 to D4. The decrease in strength with both increasing diameter and increasing gauge is also supported in the trends in the maximum force.

25
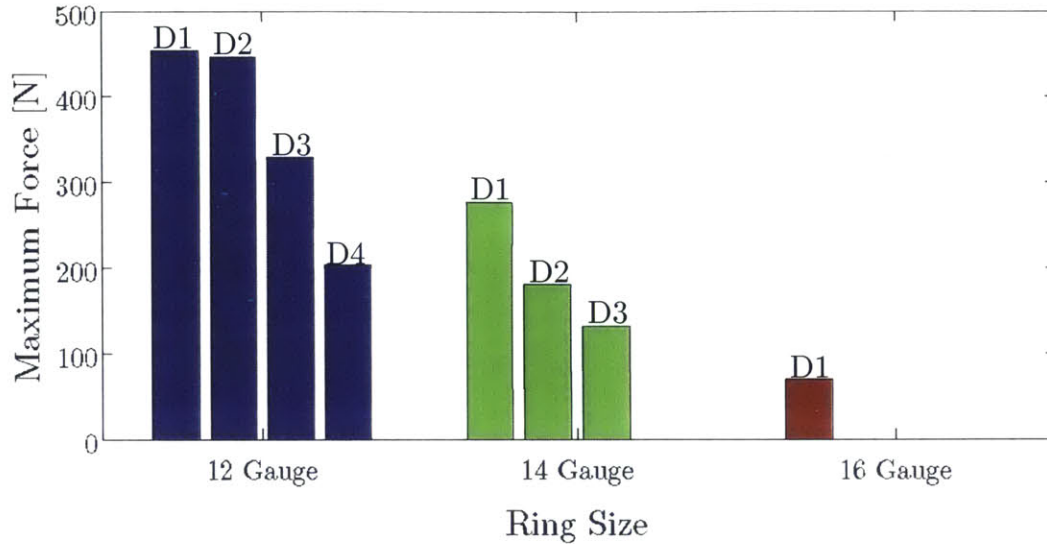
Figure 5.5: The relative maximum forces for boxes made from 12, 14, and 16 Gauge rings at the four different diameters, with the diameters ranging from D1 to D4. The decrease in strength with both increasing diameter and increasing gauge is also supported in the trends in the maximum force for the box weave.

5.3 Diameter and Gauge Proportional Relationships

5.3.1 Relationship with Diameter

The yield and maximum force values were expected to exhibit scaling with the dimensional parameters of the sample – in this case the diameter. Due to the split in the butted rings, effectively only one half of each ring supported the sample during the tensile tests. Thus, it was conjectured that the force values scale with the inverse of the diameter of the rings, such that the bigger the diameter of the ring, the weaker the chainmail sample. To verify this relationship, the yield and maximum forces values for the each of the samples with a variety of diameters and gauges were multiplied by their respective diameters. The percent differences between the resulting values are tabulated for both chain and box weaves in Tables 5.2-5.5.

Overall, the data show good support for an inverse relationship between the forces experienced by a sample of chainmail and the diameter of the rings used in the chainmail. The strongest support arises from the force and diameter data collected from chains (Tables 5.2 and 5.3), rather than the box weave samples (Tables 5.4 and 5.5). This is likely due to the fact that the chain is a simpler weave than the box; the decrease in the number of rings results in fewer possibilities for inconsistency in the dimensions of the rings that would leate to variations in the yield and maximum forces observed.

Table 5.2: Percent differences calculated between each of the yield and maximum forces found for chains made from 12-gauge rings. The majority of the difference values contained within the table are below 10% (shown in green) and so this data appears to support the conjecture that the yield and maximum forces vary with the inverse of the diameter.

Diameters Compared	%Difference: Yield	%Difference: Maximum
D1 : D2	25.1807	3.40519
D1 : D3	15.2261	2.26553
D1: D4	4.49182	6.43022
D2 : D3	13.3050	5.87062
D2 : D4	29.3855	11.6785
D3 : D4	9.32117	0.986114

Table 5.3: Comparison of yield/maximum force values for different samples of chain made from 14-gauge rings; percent differences generated by scaling each of the force or maximum values by diameter and finding the error between them. The majority of the difference values contained within the table are below 10% (shown in green) and so this data supports the conjecture that the yield and maximum forces vary with the inverse of the diameter for any gauge of wire.

Diameters Compared	%Difference: Yield	%Difference: Maximum
D1 : D2	9.89494	3.40519
D1 : D3	33.1860	2.26553
D2 : D3	47.8118	6.43022

Table 5.4: Comparison of force values via percent differences for box weave samples made from 12-gauge rings. Half of the difference values contained within the table are below 10% (shown in green) with several of the values slightly above this cut-off, and so this data shows some support for the conjecture that the yield and maximum forces vary with the inverse of the diameter.

Diameters Compared	%Difference: Yield	%Difference: Maximum
D1 : D2	12.2786	32.3553
D1 : D3	8.93301	20.5435
D1: D4	4.30244	7.73627
D2 : D3	3.81393	17.4617
D2 : D4	9.09265	59.2680
D3 : D4	5.08479	35.5914

Table 5.5: Percent difference calculations comparing force values for samples of the box weave made from 14 gauge rings. Two of the six error values contained within the table are below 10% (shown in green), while the rest of the values are between 10% and 25%. As a result, this box data shows minimal support for the conjecture that the Yield and maximum forces vary with the inverse of the diameter.

Diameters Compared	%Difference: Yield	%Difference: Maximum
D1 : D2	15.4309	2.82631
D1 : D3	23.7147	17.4757
D2 : D3	9.79535	14.2458

5.3.2 Relationship with Gauge

The yield and maximum force values were expected to exhibit scaling with another dimensional parameter of the rings in addition to the diameter – the gauge. The full cross-sectional area of the wire used to make each ring supported the load applied to each ring. Thus, it was conjectured that the force values scale with the cross-sectional area of the rings, such that the bigger the cross-sectional area of the ring, the stronger the chainmail. This hypothesis holds true for the maximum and yield forces recorded in Figures 5.2-5.5, as the forces experienced decreased with increasing gauge (decreasing thickness) for each of the sets of diameters (the group of D1s, D2s, or D3s). Although there is a relationship between the thickness of the wire and the yield and maximum forces, the nature of this relationship (linear, quadratic, etc.) is not known.

Tables 5.6 and 5.7 tabulate the attempt to scale the forces experienced by both chains and boxes with the cross-sectional area of the rings; each of the force values was divided by the square of the radius of the wire cross-section and the percent difference between each of the values for D1, D2, and D3 calculated. To correct for the slight difference in internal diameter between the rings of different gauges, the forces were also all multiplied by the internal diameter of the rings used – in accordance with the directly proportional relationship discovered in the previous section (Section 5.3.1). This correction was only used for the chains, though, due to the far higher errors in this scaling with diameter observed for the boxes in Section 5.3.1.

Table 5.6: Percent differences calculated between samples of chain made from 12 and 14 gauge rings (12G and 14G) for three of their respective diameters (D1, D2, and D3). None of the error values contained within the table are below 10% and so it appears that some behavior other than a variation with the cross-sectional area of the rings is occurring for the variation of the yield and maximum forces.

| Gauges Compared	%Difference: Yield	%Difference: Maximum
12GD1 : 14GD1	15.7138	30.8456
12GD2 : 14GD2	30.0125	35.0029
12GD3 : 14GD3	46.3512	32.0664

Table 5.7: Percent differences comparing the yield and maximum forces for 12 and 14 gauge box weave. While these error values are lower than those in table 8, only one of the error values contained within the table is below 10%, and so there appears to be little support from this data that the yield and maximum forces scale proportionally with cross-sectional area of the wire used to make the rings.

Gauges Compared	%Difference: Yield	%Difference: Maximum
12GD1 : 14GD1	19.8119	12.5806
12GD2 : 14GD2	15.6934	41.7098
12GD3 : 14GD3	7.11281	42.6200

The data collected show that as the gauge of the wire used to make the rings increases (wire thickness decreases), the yield and maximum forces decrease. However, the data appears to provide little to no support for the hypothesis that this decrease is proportional to the cross-sectional area of the wire. It is unclear if this observation is an accurate description of the behavior of the rings, or if the large error values arose from errors present in the experimentation methods (discussed in Section 7).

5.4 Effective Elastic Moduli

Each of the types of samples exhibited a different effective elastic modulus, the values of which are shown in Figure 5.6 for 12 and 14-gauge chains and boxes. While the elastic modulus found from a stress-strain graph is a material property, the effective elastic modulus found from a force-displacement curve varies as a function of the diameter of the rings. A set of linear fits for each of the groups of data is also shown on the graph. These linear fits describe the decrease in the effective modulus of elasticity as the diameter of the rings increases. The slopes found for each of the fits are tabulated in Table 5.8, along with their uncertainties, which speak to the goodness of the fits. The average rate of decrease of the effective elastic modulus with diameter (found from the values in this table) is 5.7099 ± 0.5541 N/mm. Thus, the elastic modulus is found to decrease linearly with the diameter of the rings across a variety of gauges and weaves.
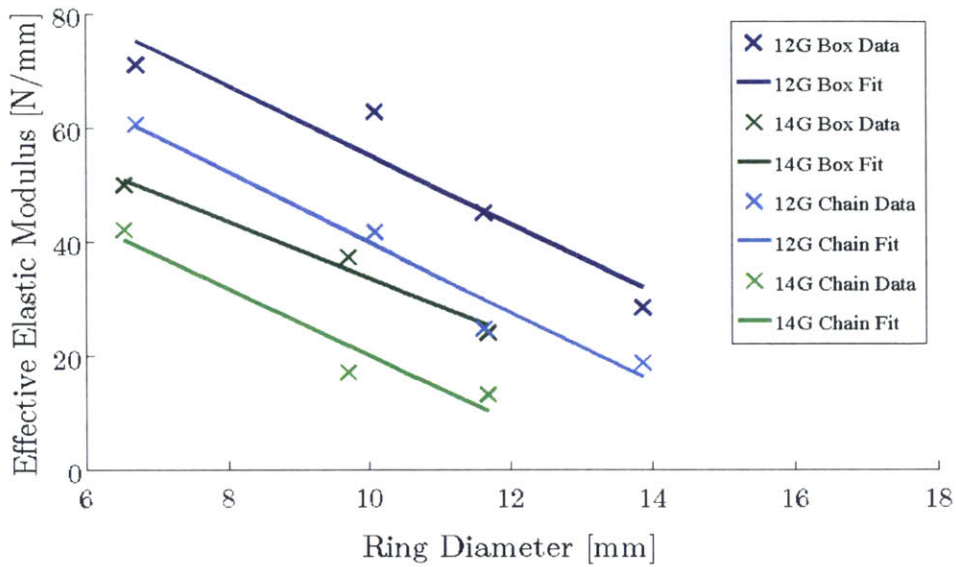
Figure 5.6: The trends in the effective Young's moduli for boxes made from 12 and 14-gauge rings with a variety of diameters. The slopes of the two appear to be comparable, with the shifts in the y-intercepts occurring due to the change in gauge or chain in weave type.

Table 5.8: Slopes of the linear fits applied to each of the sets of elastic moduli generated from 12 and 14 gauge chain and box tests at different diameters. The slopes are all relatively consistent between the weaves and gauges. The uncertainty values characterize the goodness of the corresponding linear fits.

	12-Gauge	12-Gauge Fit Uncertainty	14-Gauge	14-Gauge Fit Uncertainty
Chains	- 6.1210 N/mm^2	3.7358	- 5.7928 N/mm^2	5.0255
Boxes	- 6.0211 N/mm^2	5.9056	-4.9046 N/mm^2	2.2977

6. Experimental Results: Welded and Riveted Rings

Three samples of each of five welded sample types underwent tension tests to find the yield and maximum forces and elastic moduli for welded samples. The average yield force value and effective elastic modulus value for each sample type are shown in Figures 6.1 and 6.2. The welded and riveted samples have comparable effective elastic moduli for similar diameters and gauges of rings, but welded samples have significantly higher yield strengths. In addition, the values in the figures show similar trends to those found for butted rings in that as internal diameter of the rings increases and thickness of the rings decreases (gauge increases) the yield forces decrease. The maximum forces found for the welded rings varied significantly – between 2527.1 N and 4266.6 N – most likely due to the quality of the individual welds, and so did not exhibit any clear variation with ring dimensional parameters.

Figures 6.1 and 6.2 also show the yield force value and effective elastic modulus value for the riveted sample. The experimental results for riveted rings are limited due to the fact that samples of the riveted rings could only be purchased with one diameter and gauge. In spite of this limitation on quantity of riveted sample types, the values extracted from the force-displacement curves for the riveted sample are indicative of the strength of riveted samples. Due to the fact that the quality of the rivets in the rings was relatively uniform, unlike the welds, a maximum force value of 234.9 N was found for the riveted samples, in addition to the yield force and effective elastic modulus shown in the figures below.
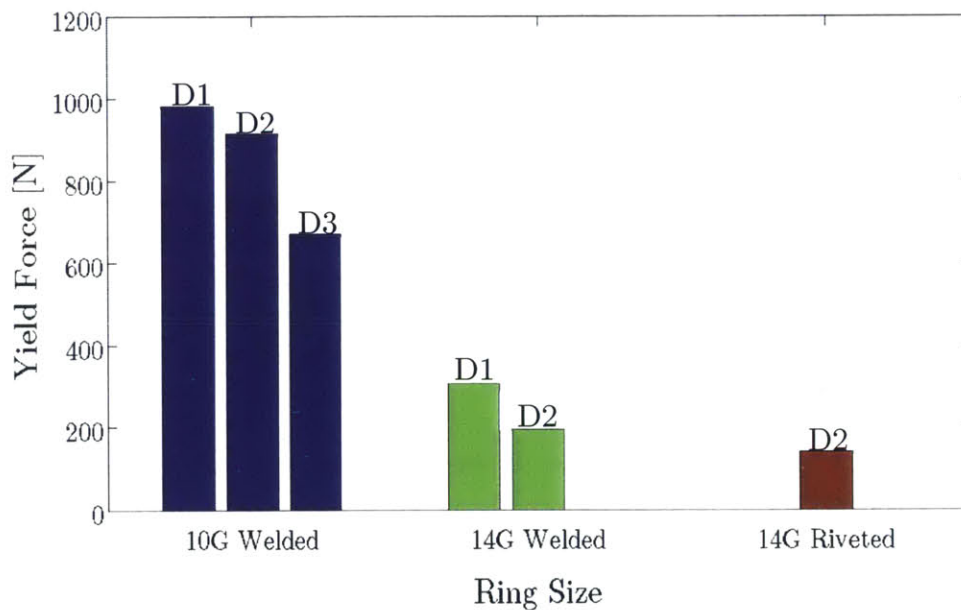
Figure 6.1: The relative yield forces for welded chains made from 10 and 14 gauge rings at three different diameters – with D1 being the smallest – and one size of riveted chains. There is a clear inverse relationship between increasing yield force and increasing diameter and gauge for the welded rings.
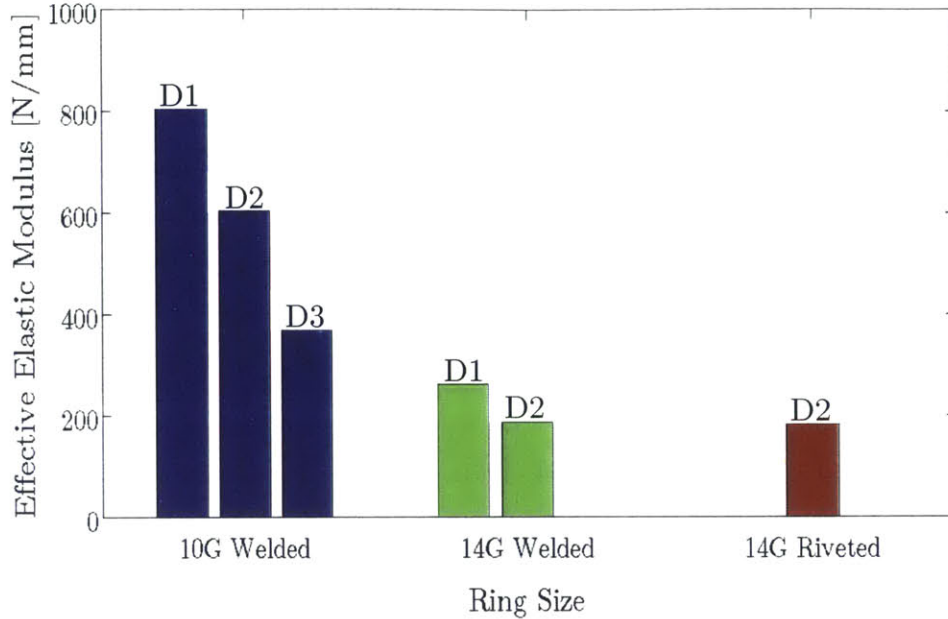
Figure 6.2: The relative effective elastic moduli for welded chains made from 10 and 14-gauge rings at three different diameters, and 14-gauge riveted chains at one diameter. There is a clear inverse relationship between increasing yield force and increasing diameter and gauge for the welded rings.

7. Sources of Experimental Error

There were a significant number of large percent difference values calculated during the investigation of how yield and maximum forces and effective elastic moduli scale with diameter and gauge. The magnitude of the quantifiable errors for each of the force values or effective Young's moduli was on the order of 0.1% (as so is practically invisible on the figures). The quantifiable errors factored into this calculation were the uncertainty in the ring diameter and ring radius and the error in the INSTRON machine measurements. If the scaling attempted with both ring diameter and cross-sectional areas is assumed to be true, this 0.1% is insufficient to explain the large percent differences calculated between many of the values being compared.

There exist a number of significant sources of error resulting from the sample construction and positioning of the rings during testing. One potentially large source of error was the orientation of the opening of the butted rings. Based upon the initial placement of the opening, the rings could have been more or less likely to slip through one another before much plastic deformation had occurred. The orientation of the closure point on the rings would have also impacted the behavior of the riveted samples, as the closure point remained a weaker area of the sample (unlike in the welded samples which did not consistently fail at the weld). This could explain much of the error in the

maximum force values for the butted and riveted rings. Additionally, there existed some variation between the samples due to the fact that they were made by hand. In the case of the butted rings, the size of the opening of the ring would have had a large impact on the likelihood of slippage of the rings as well as the degree of plastic deformation that needed to occur in order for the rings to fail. Similarly, the width of the welded area and size of the rivet could also have impacted the strength of the sample. These experimentally non-quantifiable errors could have had a significant impact on both the values of the yield and maximum forces.

A potential source of error impacting both the maximum and yield forces and the effective elastic modulus was that due to the nature of the testing rig or the shape of the chainmail, some of the samples were at a slight angle in the machine. This would have resulted in the application of a not purely tensile force, which would impact the values in the force-displacement graph for all of the types of samples. Thus, there are a number of errors difficult to quantify experimentally that could explain the large percent differences between some of the values being compared in the scaling analyses.

8. Simulation Results and Discussion

Values found experimentally were used to verify the accuracy of yield force and effective elastic modulus values output by SolidWorks simulations. These simulations were then used to investigate several of the possible sources of experimental error and analyze the impact that these errors could have on the experimental results.

8.1 Simulation Outputs

The SolidWorks simulations accepted a force value imposed on the top face of the feature added to the top ring and gradually ramped up the force applied until it reached this value. At the end of each simulation, stress, displacement, and strain profiles, along with force values, were generated. An example of a stress profile experienced by the simulated rings is shown Figure 8.1. This stress profile followed the predicted zones of highest and lowest stress in the rings, providing qualitative verification of the validity of the SolidWorks simulation.

Figure 8.1: Image of the stress profile in the rings generated by a SolidWorks simulation of 12-gauge, D2 butted rings with a 0.3mm gap at the 90° position. Stress is concentrated at the fixed feature at the bottom, the feature that the force was applied to at the top, and in the middle of the bend in the ring. Additionally, very little force is experienced by the side of the ring with a split in it.

In order to find the yield forces and elastic moduli of the simulated samples, force-displacement graphs were generated from the simulation data. Due to the fact that the SolidWorks simulation package used was not sophisticated enough to process high levels of plastic deformation, the form of the output graph was bi-linear. The initial linear region of the force-displacement graphs generated simulated the elastic deformation of the sample. Thus, the slope of this portion of the graphs gave the effective elastic modulus of the sample. This value was then multiplied by a factor of 4.5 to account for the fact that the simulated samples were 4.5 times shorter than the experimental samples. The force-displacement graph entered its second linear phase at the yield point of the material. Thus, a yield force could be found, but no maximum force. Examples of the force-displacement graphs generated by the SolidWorks simulations are given in Figures 8.2 and 8.3.
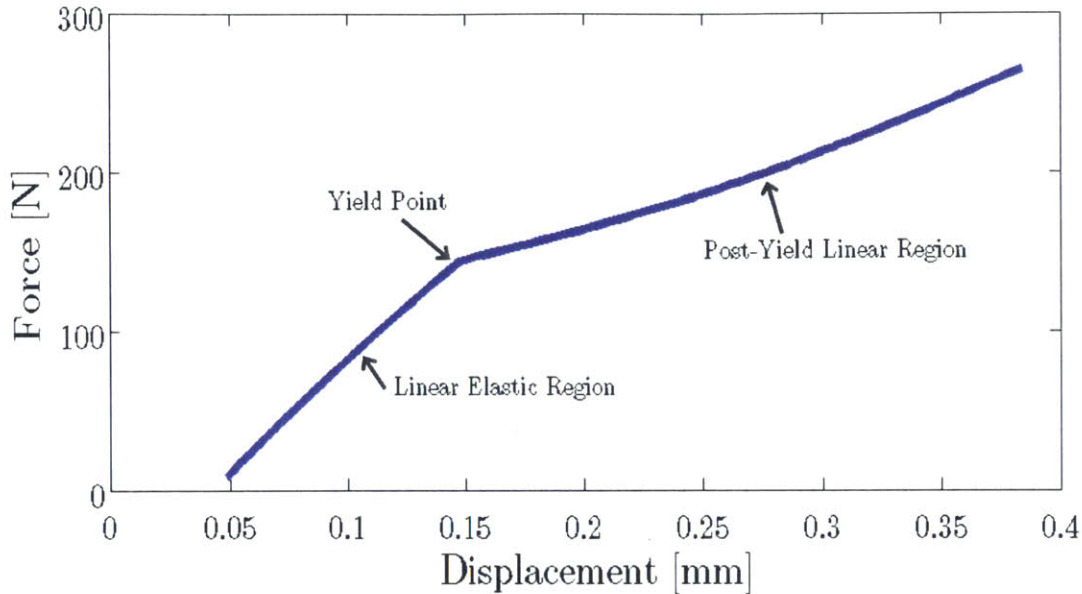
Figure 8.2: An example of the bi-linear graphs created by the SolidWorks simulations for a 12 gauge, D2 sample with a split width of 0.001 mm. The graphs clearly displays an initial elastic region, a kink in the curve at the yield force and a second linear region after the yield force has been achieved.
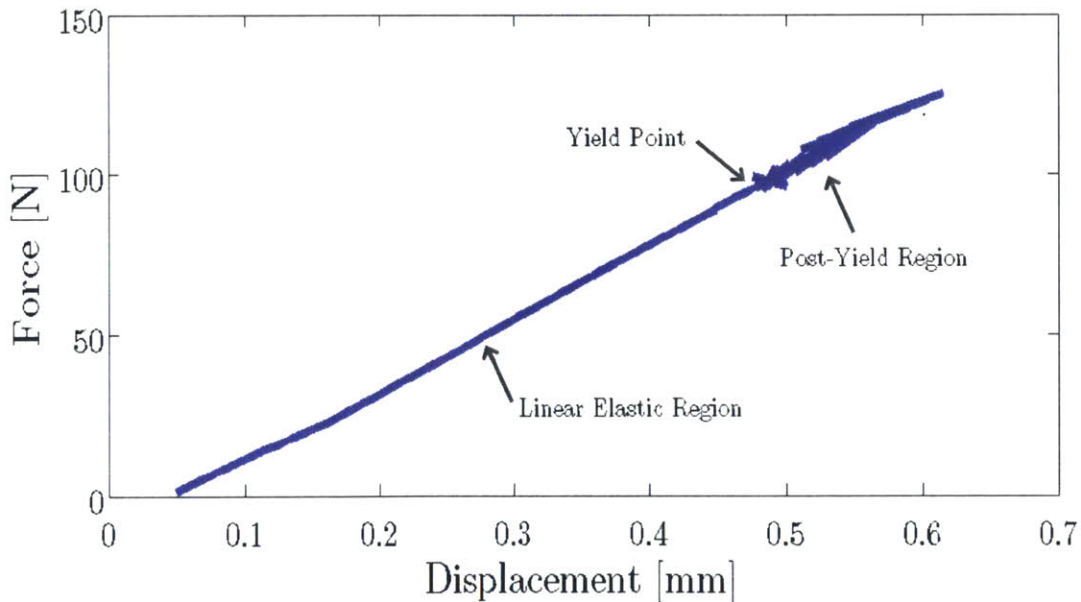
Figure 8.3: A second example of the graphs created by the SolidWorks simulations for a 12 gauge, D2 sample with a split width of 0.3 mm. Compared to Figure 20, which exhibits a clear bi-linear trend, this curve begins to double back on itself around 100 N. Due to the fact that the SolidWorks simulation package has difficulty handling plastic deformation, the last point in the curve before any doubling-back occurred was assumed to be the yield point of the sample.

8.2 Verification of Simulation Results

The yield force and effective elastic modulus values found using the simulation were compared to the corresponding experimental values to verify that the values were similar. The comparative yield values for a slection of the experimental and simulated welded, butted, and riveted samples is shown in Figure 8.4 and the errors between those values shown in Table 8.1. Contained within the figure and table are two butted and two welded samples with different gauges and (slightly) different diameters. The values for a simulated riveted sample with the same dimensions as the physical samples is also included. Figure 8.5 and Table 8.2 contain the effective elastic modulus values corresponding to each of these same combinations. The high levels of agreement between the simulated and experimental Young's modulus and yield force values reinforce the ability of the simulations to accurately model a set of two chainmail rings.
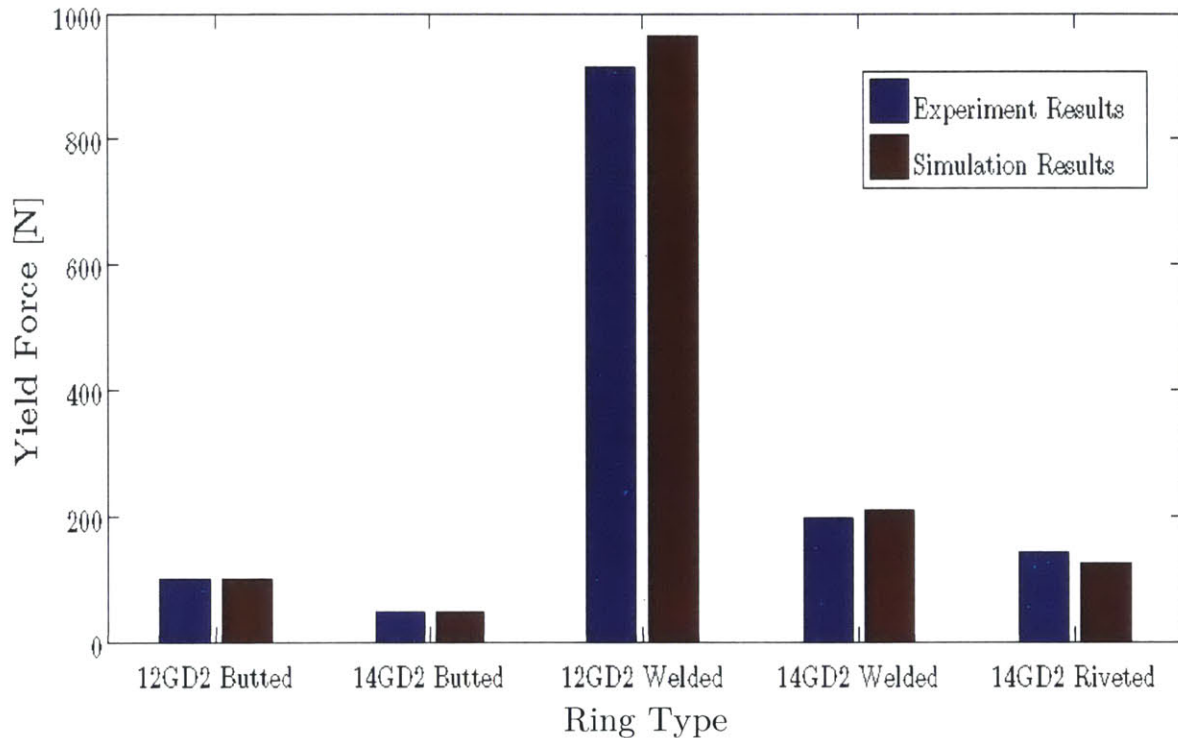
Figure 8.4: A comparison of the experimental and simulated values for a variety of different gauges and diameters and ring closure methods. All of the experimental and simulated values shown appear to match relatively well with the corresponding simulated/experimental values.

Table 8.1: The errors between the corresponding simulated and experimental yield force values shown in Figure 26. The values for the welded and butted rings (shown in green) are significantly lower than 10% error, and the riveted value is very close to this imposed cut-off value.

	12GD2 Butted	14GD2 Butted	12GD2 Welded	14GD2 Welded	14GD2 Riveted
Percent Difference	- 1.570	0.027	- 5.310	- 7.340	11.39
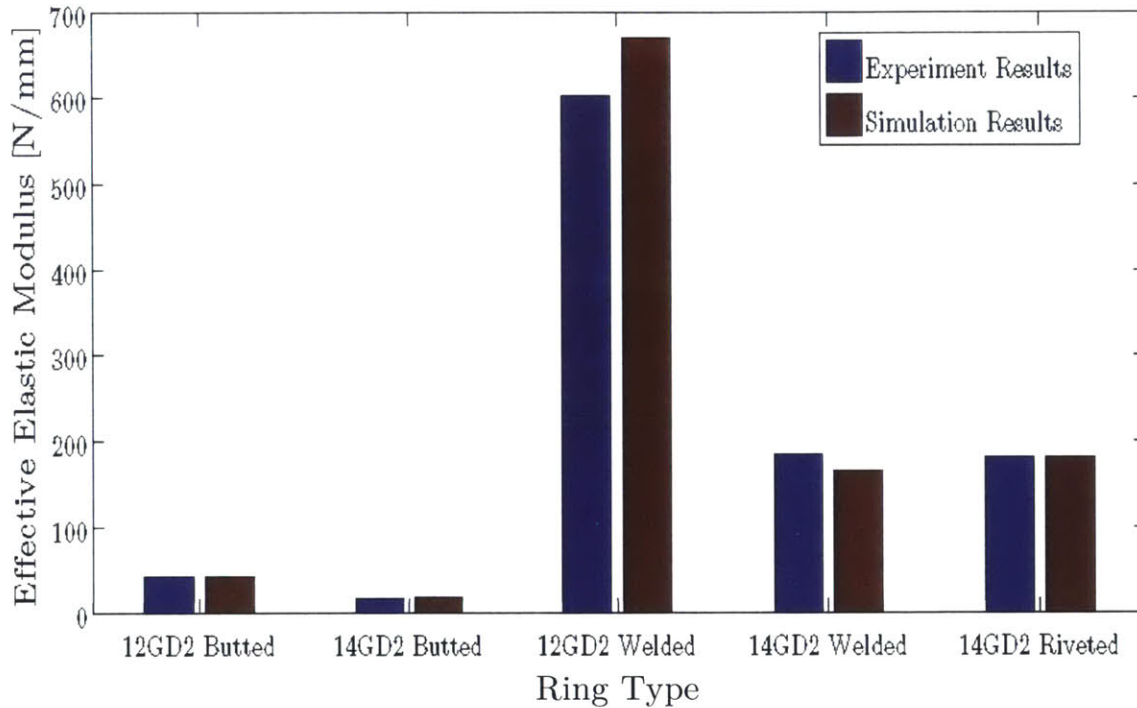
Figure 8.5: A comparison of the experimental and simulated effective elastic modulus values for a variety of different gauges and diameters and ring closure methods. All of the experimental and simulated values shown appear to match relatively well with the corresponding simulated/experimental values.

Table 8.2: The errors between the corresponding simulated and experimental effective elastic modulus values shown in Figure 25. Three of the values (shown in green) are significantly lower than 10% error, and the two that are not below this cut-off are very close to it.

	12GD2 Butted	14GD2 Butted	12GD2 Welded	14GD2 Welded	14GD2 Riveted
Percent Difference	- 0.250	- 11.14	0.120	10.36	0.880

37

8.3 Comparison of Closure Methods via Simulation

Figures 8.4 and 8.5 also aid in the visualization of the relative strengths of welded, riveted, and butted chainmail samples. Figure 8.4 reveals that for 14-gauge rings, the riveted sample yields at approximately two and a half times the force at which the butted ring sample yields, and the welded at approximately four times the force. When 12-gauge rings are used, the multiplication factor in the yield strength between the butted and welded samples is approximately twelve. As a result, an improvement in the strength by a factor of at least two, and potentially much more, occurs when the openings in the butted rings in a chainmail piece are welded or riveted closed. This improvement in the yield force likely arises from the fact that the weld and rivet allow the ring to be supported by the metal on both the left and right sides of the o-shape in the ring – unlike the butted rings in which all the force is concentrated in one side of the o-shape.

Figure 8.5 aids in the visualization of the effect that the method of closure has on the effective elastic modulus of each of the samples. The effective elastic moduli of the welded and butted rings are comparable and approximately three times the value of those for the butted rings. The similar effective elastic moduli of the welded and riveted rings is likely also brought about by the doubling of the support area for the rings with these methods of closure. Thus, until the yield point, both the welded and riveted rings behave similarly. However, the two samples types differ drastically in terms of their maximum forces; the rivet fails shortly after the yield point, while the welded sample is able to undergo significantly more plastic deformation and experiences strain hardening. This results in a maximum force on the order of 3000 N for the welded samples and 240N for the riveted samples. Overall, the butted rings are significantly weaker than the welded and riveted rings, while the riveted and welded rings behave similarly up to the yield point of the material.

8.4 Investigating Sources of Error

Posited sources of error for the butted ring tests investigated using the simulations were the orientation of the split in each of the butted rings and the width of the split. While not all encompassing, these investigations are indicative of the magnitude of possible errors in yield forces, maximum forces, and effective elastic moduli resulting from variations in sample orientation and inconsistencies in the construction of the samples.

8.4.1 Butted Ring Split Orientation

Simulated sets of two butted rings with varying diameters were chosen to investigate the impact of the orientation of the rings on the forces experienced. The

rings were simulated at the extremes of their possible orientations and at the average position, ie. the 0°, 90°, and 180° orientations shown in Figure 3.5. The gap width was set at 0.3 mm wide and the cuts made to create the 0° and 180° orientations were both offset from the vertical by one half of the width of the ring wire. The results of these simulations are contained in Figure 8.6.
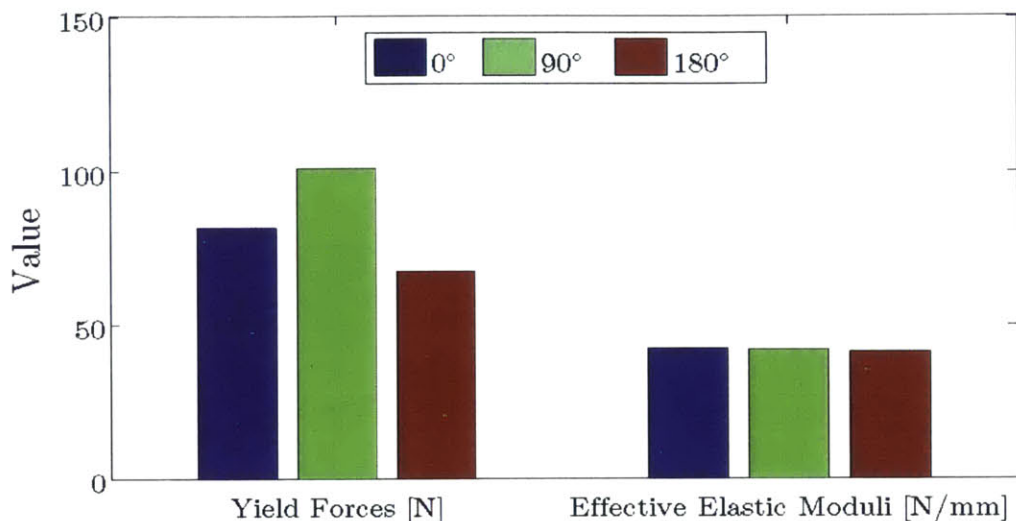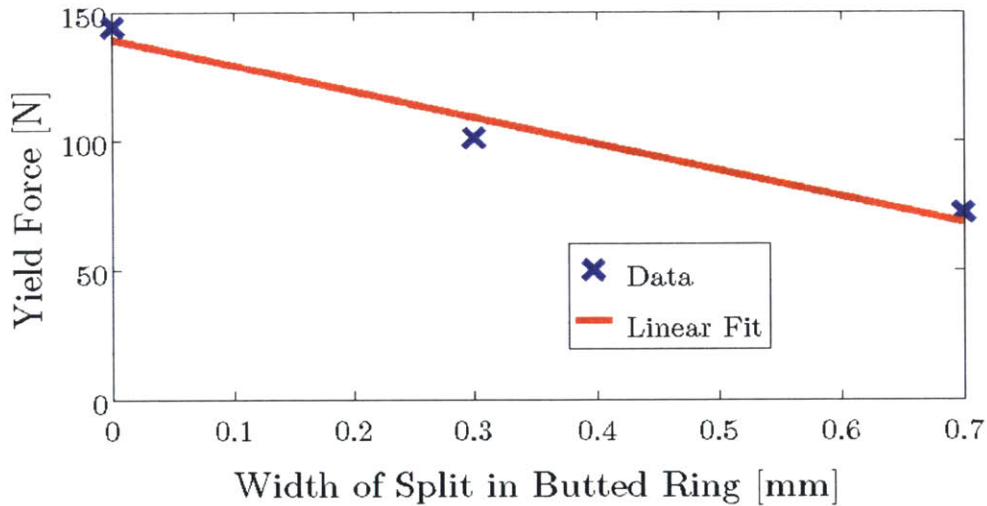

Figure 8.6: A comparison of the yield forces and effective elastic moduli found via simulation of butted ring samples with different orientations of the splits in the rings. The elastic moduli appear to be relatively consistent with one another, while the yield force values vary significantly between the different orientations.

The fact that the effective elastic moduli, which are functions of the ring diameter, ring gauge, and chain length, are highly consistent with one another lends credibility to the data, as these three parameters were unchanged between the tests. The yield force values were found to vary from the 90° value by 33.31% and 19.05% from the 0° orientation to the 180° orientation (respectively). The maximum possible change in value in the force resulting from this is 33.31% - a value similar to many of the percent differences found between the scaled force values during the investigation of how chain and box strength scale with diameter and gauge. Thus, the simulation proved the orientation of the split in the rings to be a possible source of error in the yield (and likely maximum force) values found experimentally. Due to the fact that the riveted rings consistently failed at the rivet (the analog to the split in the rings) a similar relationship likely holds true for the riveted rings. The same cannot be said with certainty for the welded rings due to the fact that the welded rings did not consistently fail at the weld in experimentation.

8.4.2 Width of Butted Ring Split

In addition to the orientation of the split in the ring, another possible source of error was the width of the split in the butted rings. Two ring chains of 12 gauge, D2 butted rings with a split oriented at 90° and three different split widths of 0.7 mm, 0.3 mm, and 0.001 mm were simulated, resulting in Figure 8.7. The linear fit shows a decrease in the yield force value of 100 N for every 1mm of gap between the ends of the rings. As with the elastic modulus values found during investigation of the ring orientation width, the effective elastic moduli were all relatively constant between the different gap widths – with a value of approximately 41 N/mm. Thus, the hypothesis that the split width impacts the forces experienced by the samples is supported by the simulation.

Figure 8.7: A comparison of the yield forces found via simulation of butted ring samples with widths of the splits in the rings. The yield force values vary significantly between the different split widths, exhibiting a linear fit with a slope of - 100 N/mm.

9. Conclusions

A series of tensile tests was conducted on samples of chainmail with seven different diameters, four gauges, and four weave types, to create force versus displacement graphs for each of the samples. The effective elastic moduli, yield forces, and maximum forces of chainmail (found graphically) vary based upon factors including the type of chainmail weave, the diameter of the rings, and the gauge of the rings. It was determined that the yield and maximum forces of the chainmail vary directly with the number of rings passing through each ring and inversely with the radius of the rings. The effective elastic modulus (which relates to a sample's resistance to elastic deformation) of each of the samples was also found to decrease with increasing diameter at a rate of -5.7099 ± 0.5541 N/mm^2. The attempt to also scale these forces with the

40

cross-sectional area of the rings proved inconclusive due to large differences between the values compared. Thus, some success was achieved at correlating the parameters of a chainmail weave to the behavior of the sample when it is subjected to tension.

Further experimentation was conducted into how the method of closure of the rings impacts the strength of a chainmail sample by comparing the yield and maximum forces and effective elastic moduli of butted, riveted and welded samples. Three diameters and two gauges of welded rings were tested along with one diameter and gauge of riveted rings. The effective Young's moduli of the welded and riveted rings were approximately six times that of the butted rings. The yield forces of the riveted rings and welded rings were at least two times the values of the yield forces for the butted rings. The maximum forces varied more significantly between different samples of the welded and riveted chains due to the inconsistencies in the qualities of the rivets and the welds. However, the maximum force that the rivets were capable of withstanding was 20% that of the welded rings and at least 150% that of the butted rings. Thus, relative strengths of the butted, riveted, and welded chainmail samples were established.

Non-linear, dynamic SolidWorks simulations were also conducted for a variety of chain types. The accuracy of the simulations was verified by comparing the output yield forces and effective elastic moduli to the values found experimentally; the majority of the values differed by well under 10% and so the SolidWorks simulations were shown to be a sufficiently accurate reproduction of the physical testing. This verification allowed for the investigation of several possible sources of error in the data collected experimentally – namely the width of the gap in the butted rings and the orientation of the gap. Using the simulations, the orientation of the split in the ring was found to be capable of inducing variations in the data of up to 33.31%, which is on the order of a number of the differences between the values compared in the analyses of the butted rings. Additionally, the width of the split in the rings led to a decrease in the yield force of 100 N per millimeter of increase in the width of the split. The ring opening size and orientation is analogous to the rivet location and orientation and the weld thickness, so the verification of these sources of error indicate that the values found for riveted and welded samples could have been similarly affected. Thus, possible explanations were found for some of the large percent difference values and deviations from the expected proportional relationships found in earlier experiments.

10. References

[1] Williams, Alan. "The Manufacture of Mail in Medieval Europe: A Technical Note." 1980. Web. 1 Feb. 2015.

[2] "AISI 1018 Mild/Low Carbon Steel." *AZO Materials.* Web. 1 May 2015.

[3] "Galvanizing – Affect on Steel Strength." *AZO Materials.* Web. 1 May 2015.

[4] Aifantis, Elias. "The Physics of Plastic Deformation." *The International Journal of Plasticity* 3.3 (1987): 211-47. *Science Direct.* Web. 1 April 2015. <http://www.sciencedirect.com/science/article/pii/0749641987900210>.

[5] *Chain.* Digital image. *Source: http://www.goldenlighting.com/Chain-7644-GA_zoom.jpg.* 1 April 2015. Web.

[6] Spiral Weave. Digital Image. Source: https://metalandmineral.files.wordpress.com/2011/10/spiral.jpg. 1 April 2015. Web.

[7] *European Weave.* Digital Image. *Source: http://cdn.instructables.com/FOH/OLIS/HO7XFLHF/FOHOLISHO7XFLHF.LARGE.jpg.* 1 April 2015. Web.

[8] *Jump Ring.* Digital Image. *Source: http://images.artbeads.com/colored-split-rings-find-1117-sm.jpg.* 1 April 2015. Web.